Anomalous Mass Transport in the Pb Wetting Layer on the Si(111) Surface

K. L. Man,[1] M. C. Tringides,[2] M. M. T. Loy,[1] and M. S. Altman[1]

[1]*Department of Physics, Hong Kong University of Science and Technology, Clear Water Bay, Kowloon, Hong Kong, China*
[2]*Ames Laboratory-USDOE and Department of Physics and Astronomy, Iowa State University, Ames, Iowa 50011, USA*

(Received 1 September 2008; published 26 November 2008)

The temporal evolution of nonequilibrium coverage profiles in the Pb wetting layer on the Si(111) surface is studied using low energy electron microscopy. The initial coverage step profile propagates rapidly at a constant velocity with an unperturbed shape. A model is proposed that attributes this nonclassical equilibration behavior to the diffusion of thermally generated adatoms on top of the wetting layer. This model can account for the observed convectionlike mass transport, as well as its dramatic dependence on Pb coverage. Such anomalous mass transport is believed to facilitate the remarkably efficient self-organization of uniform Pb quantum island height on the Si(111) surface that was observed previously.

DOI: 10.1103/PhysRevLett.101.226102 PACS numbers: 68.43.Jk, 68.35.Fx, 68.37.Nq, 68.65.Fg

The capability to control the dimensions of nanostructures is essential for varying and controlling their electronic structure and properties. Recent experiments have shown that it is possible to exercise control over the height of metallic islands on various substrates by exploiting quantum size effects (QSEs) in film energetics that are caused by electron confinement [1–8]. However, kinetic growth limitations may interfere with the control over morphology that is promised by QSE-driven energetics [7]. The formation of stable, uniform height Pb islands on the Si(111) surface is an excellent example of this intriguing QSE phenomenon [5,9–13], particularly because an extremely sharp height distribution is obtained rapidly at very low temperature. Although QSEs in diffusion kinetics *on top* of Pb quantum islands on Si(111) have also been reported [14,15], this aspect of kinetics cannot explain the remarkable efficiency of the self-organization of island height in this system.

Recent experiments [16,17] that shed light on this issue have shown that the dense Pb wetting layer that forms on Si (111) prior to island nucleation plays a crucial role in the self-organization. Observations of island growth and coarsening suggested that the wetting layer transfers material collectively to islands, not by independent diffusion events, but apparently by its continuous spreading. Despite these intriguing observations, wetting layer diffusion and mass transport are not fully understood because of the lack of direct and comprehensive measurements of these phenomena.

In this Letter, we report the results of such direct measurements that were made using low energy electron microscopy (LEEM). Information on mass transport is obtained here from observations of the temporal evolution of nonequilibrium coverage profiles that are prepared by laser induced thermal desorption (LITD). Diffusion experiments are often carried out by monitoring the relaxation of spatial coverage gradients [18–20], generated either by equilibrium fluctuations or imposed externally. Since the diffusion equation is a differential equation of second order in the space variable, r, and first order in the time variable, t, it predicts that an evolving coverage profile, $\theta(r, t)$, is only a function of the scaled variable $\eta = r^2/t$. Similar scaling is naturally found in the temporal evolution of the fourier components for any initial profile. Each component decays exponentially with a unique time constant that is inversely proportional to the product of the diffusion coefficient, D, and the square of wave vector, k. Consequently, large k components are suppressed faster than small k components. This gives rise to classical profile broadening and a gradual approach to equilibrium uniform coverage distribution that is scaled in time by D.

Real-time LEEM observations of profile evolution in Pb/Si(111) reveal several surprising features that are at odds with this classical behavior. Not only is the wetting layer extremely mobile, we find that the initial coverage step profile that is produced by LITD propagates from the edge of the desorption region at approximately constant velocity and with largely unperturbed profile shape. This points to an unconventional convectionlike mass transport. The dependence of the equilibration time on initial Pb coverage also exhibits an intriguing threshold behavior, characterized by an exceptionally sharp divergence below a critical coverage, θ_c. These observations give important clues about the nature of mass transport in the Pb wetting layer on Si(111).

The experiments were carried out in a low energy electron microscope. In LEEM, a surface is imaged using elastically backscattered electrons in the specular diffraction beam. LITD uses a single laser pulse to desorb atoms or molecules by heating the substrate locally. LITD is carried out here using a pulsed Nd:YAG laser ($\lambda =$ 1064 nm) with 10 nsec pulse width [19]. Experiments were performed on two different Pb phases on the Si (111) surface: the amorphous wetting layer on the clean (7×7) surface reconstruction and the weakly bound Pb-α $(\sqrt{3} \times \sqrt{3})$ wetting layer (the α-phase) that is formed by

annealing the amorphous layer. The ideal α-phase coverage is $\theta = 4/3$ monolayer (ML) [21].

Illumination of the Pb-covered surface with a single laser pulse causes desorption of Pb from a nearly circular region. LEEM images that show the surface immediately before and after LITD from the α-phase are presented in Fig. 1. Calibration of the Pb coverage profile produced by LITD was made by measuring the LEEM image intensity while redepositing Pb at 120 K. At this temperature, Pb diffusion from the edge of the desorption region, or hole, is suppressed. The LEEM image intensity increases approximately linearly within the hole during redeposition up to a peak at 4/3 ML. This linearity means that the spatial intensity profile is a good representation of the Pb coverage profile within the LITD hole. The amount of redeposited Pb that is required to reach the intensity peak at each point is taken to be equal to the amount of Pb that was desorbed locally. This treatment reveals the presence of a sharp coverage discontinuity at the edge of the hole initially and the shape of the initial profile within the hole [Fig. 1(e)]. The amount desorbed at the center varies linearly between 0.4 ML and 1.0 ML for hole radii in the range from 5 to 25 μm, controlled by the laser pulse energy. LITD of more than 1 ML is apparently inhibited by the emergence of the strongly bound Pb-β $(\sqrt{3} \times \sqrt{3})$ phase, which forms ideally at a coverage of 1/3 ML [22]. This produces a flat bottom coverage profile for radii exceeding 25 μm.

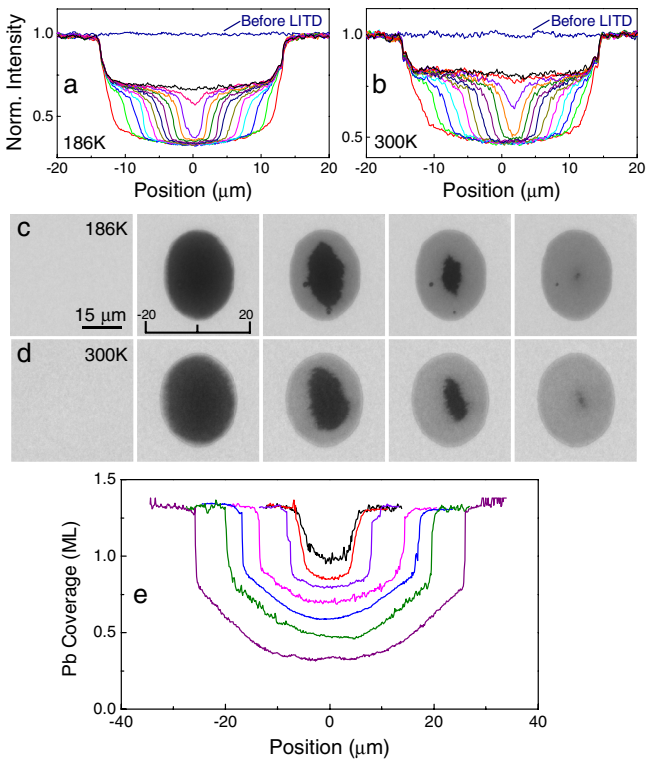

FIG. 1 (color online). Profile evolution in the Pb α-phase on Si (111) following LITD for $\theta > \theta_c$ at (a), (c) $T = 186$ K and (b), (d) $T = 300$ K. The time intervals between LEEM intensity line profiles in (a) are $\Delta t = 4.1$ sec and in (b) are $\Delta t = 0.2$ sec. LEEM images are shown (l. to r.) in (c) at times $t = 0$, 0.8, 15.7, 30.5, 45.4 sec, and in (d) at $t = 0$, 0.01, 0.8, 1.4, 2.0 sec. The initial LITD coverage profiles determined from Pb redeposition experiments at 120 K for different LITD hole radii are shown in (e).

The appearance of the β-phase is confirmed by low energy electron diffraction (LEED). A single laser pulse produces an abrupt increase in the $(\sqrt{3} \times \sqrt{3})$ diffraction intensity, indicating the formation of the β-phase. At temperatures where diffusion occurs, the β $(\sqrt{3} \times \sqrt{3})$ pattern is transient. Measurements of LEED intensity vs energy, $I(V)$, which are indicative of surface structure, were also performed with diffusion suppressed at 120 K. The $I(V)$ spectra within the LITD hole exhibit unique features that are characteristic of the β-phase that is produced by conventional thermal desorption of excess Pb. The LEEM and LEED experiments therefore show consistently that up to 1 ML of Pb is removed easily from the weakly bound α-phase by LITD. The limit to the desorbed quantity, imposed by the emergence of the strongly bound β-phase, is equal to the coverage difference between the two phases.

The equilibration of the Pb coverage profile produced by LITD is illustrated in Fig. 1. LEEM image series and corresponding image intensity line scans through a diameter of the desorption region at 186 and 300 K are shown. These data clearly reveal an abrupt step profile that propagates from the edge of the desorption region at approximately constant velocity and with approximately constant shape. These observations are most unusual because they do not conform to the classical behavior, which is characterized by profile broadening during gradual equilibration. Note that the lower intensity that is observed within the LITD hole after equilibration can be attributed to disorder that is introduced during rapid mass transport. Reordering and the full recovery of intensity are achieved by slight post-annealing.

Considering that the coverage step profile advances at constant velocity during equilibration, we adopt the equilibration or hole filling time, τ, for fixed hole radius as a measure of kinetics. The filling time exhibits a very dramatic dependence on the (initial) coverage in the surrounding area [Fig. 2(a)]. Above a critical coverage, $\theta_c \sim 4/3$ ML, τ is independent of coverage within experimental uncertainty. The temperature dependence of $1/\tau$ for $\theta > \theta_c$ also exhibits a clear Arrhenius behavior corresponding to a low activation barrier of 0.15 eV [Fig. 2(b)]. However, τ increases very sharply below θ_c with a pronounced exponential coverage dependence, $\sim \exp[\kappa(\theta_c - \theta)]$, where κ exceeds 100 ML^{-1}.

In order to understand mass transport in this system, we first consider the possible coverage dependence of the diffusion coefficient, $D(\theta)$, which is known to influence profile evolution behavior. This influence is exploited in the Boltzmann-Matano (BM) analysis method of profile evolution to determine $D(\theta)$ [20]. According to the BM

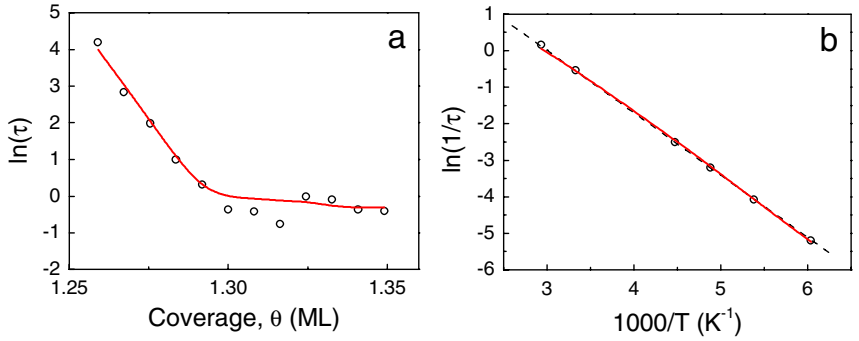

FIG. 2 (color online). The dependence of the equilibration time, τ, for LITD hole radius of 17 μm upon (a) the initial wetting layer coverage, θ, at 341 K and (b) temperature for $\theta = \theta_c$. The dashed line in (b) is the Arhennius law with activation energy 0.15 eV. The solid lines are model predictions (see text).

method, the sharp step profile shape for Pb/Si(111) suggests a strong coverage dependence of diffusion. Coverage dependent diffusion must also be accountable for the steep exponential divergence of τ below θ_c. While this in itself would be exceptional, modeling using the diffusion equation with $D(\theta)$ cannot reproduce the τ divergence consistently with the invariant step profile shape at all T, $\theta > \theta_c$ and $\theta < \theta_c$. Therefore, it appears that some other mechanism is responsible for the puzzling equilibration behavior.

As an alternative explanation, we propose that mass transport occurs due to diffusion of thermally generated adatoms on top of the wetting layer. It is reasonable to expect that adatom-vacancy pairs can be created in the Pb wetting layer because it is compressed compared to the closed-packed Pb(111) surface layer (equivalent to $\theta =$ 1.2 ML on Si(111)). We denote the adatom concentration as $c_{\mathrm{ad}}(r, t)$, the vacancy concentration as $c_{\mathrm{vac}}(r, t)$ and the local wetting layer coverage as $\theta(r, t)$, and express the adatom-vacancy creation and annihilation rates as $R_c\theta$ and $R_a c_{\mathrm{ad}} c_{\mathrm{vac}}$, respectively. The rate constants are related to attempt frequencies and activation barriers by $R_c = R_{c0}\exp(-E_c/kT)$ and $R_a = R_{a0}\exp(-E_a/kT)$. The following rate equations describe the time evolution of the concentrations of the three species under the assumption that only adatoms are mobile with diffusion coefficient $D_{\mathrm{ad}} = D_0\exp(-E_D/kT)$:

$$\frac{\partial c_{\mathrm{ad}}(r, t)}{\partial t} = D_{\mathrm{ad}}\nabla^2 c_{\mathrm{ad}}(r, t) + [R_c\theta(r, t) - R_a c_{\mathrm{ad}}(r, t)c_{\mathrm{vac}}(r, t)], \quad (1a)$$

$$\frac{\partial\theta(r, t)}{\partial t} = -\frac{\partial c_{\mathrm{vac}}(r, t)}{\partial t} = -[R_c\theta(r, t) - R_a c_{\mathrm{ad}}(r, t)c_{\mathrm{vac}}(r, t)]. \quad (1b)$$

In steady-state, i.e., before LITD, all three concentrations are spatially uniform and time-independent. The net creation-annihilation rate (C-A) term in the square bracket is correspondingly zero. This defines equilibrium adatom and vacancy concentrations, $\bar{c}_{\mathrm{ad}} = \bar{c}_{\mathrm{vac}}$, that are equal because of pair creation and annihilation. However, immediately after LITD, a spatially nonuniform wetting layer concentration, $\theta(r, 0)$, exists with discontinuity at the hole edge [Fig. 3(a)], which imparts a corresponding spatial dependence to the vacancy and adatom concentrations [Fig. 3(a) and 3(b), respectively]. This drives the diffusion of adatoms from the exterior to the edge of the hole, where they recombine with excess vacancies and move the edge

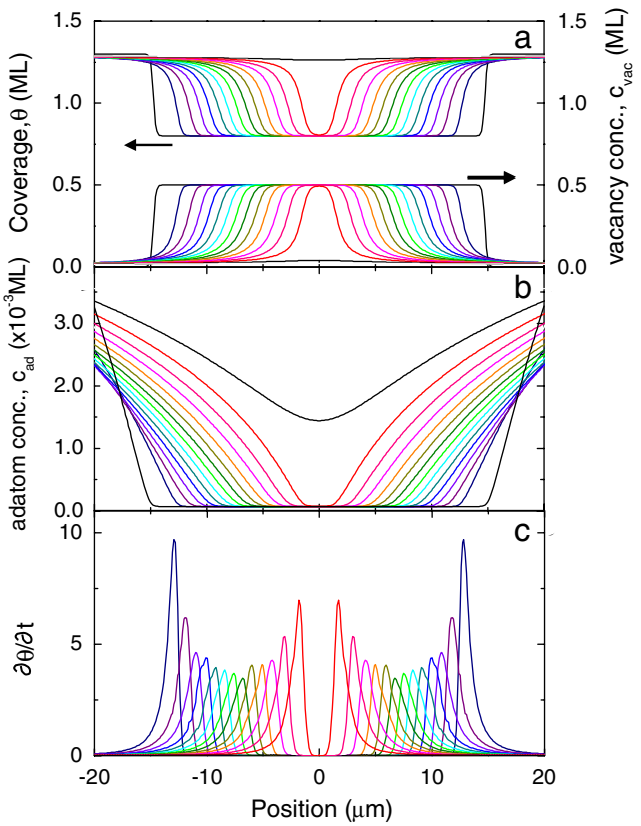

FIG. 3 (color online). Numerical solutions of the adatom-vacancy model for the radial profile evolution at 186 K of (a) the wetting layer coverage, $\theta(r, t)$, and the vacancy concentration, $c_{\mathrm{vac}}(r, t)$, (b) the adatom concentration, $c_{\mathrm{ad}}(r, t)$, and (c) creation-annihiliation term in Eq. (1), $\sim\partial\theta/\partial t$. The time interval between profiles is $\Delta t = 3.1$ sec. The optimized model parameters are stated in the text.

closer to the hole center. The profile shape at the edge remains unchanged as it moves because only at the edge is the net C-A rate nonzero [Fig. 3(c)]. Thus, the C-A term in Eq. (1b) acts as a convection term, which has the general form $\sim d\theta/dr$, because it is nonzero only at the edge where θ varies spatially. Away from the edge, the balance of creation and annihilation defines local equilibrium. This model is able to explain the experimental observations at all temperatures. For example, Fig. 3 shows the profile evolution predicted by the model calculation at 186 K for the set of parameters $E_a = 0.2$ eV, $E_c = 0.36$ eV, $E_D = 0.05$ eV, $R_{a0} = R_{c0}$. The agreement with the experimental results is excellent with regard to the step profile shape, its approximate constant propagation velocity (Fig. 1), and the temperature dependence of the equilibration time [Fig. 2(b)]. This model can also account for the coverage dependence of τ if one assumes that the creation energy increases below θ_c. A linear increase of E_c by 0.55 eV/0.1 ML produces the observed exponential divergence of τ [Fig. 2(a)]. This coverage dependence may reflect the change of stress in the wetting layer as the coverage decreases below θ_c. The nature of Pb intralayer interactions versus interaction with the underlying substrate could also play a role. Further investigations are needed to confirm and understand this effect.

We now explore the possible link between our results and observations in previous Pb quantum island growth experiments that suggest an unusually fast mass transport mechanism involving the dense Pb wetting layer, either amorphous or α-phase [16,17]. In those experiments, wetting layer mobility was detected by the fast formation of atomic height rings on the top of unstable height islands. The formation speed of the rings at 190 K was determined to be 15 nm/sec. This is the same order of magnitude as the velocity of the coverage profile edge, 45 nm/sec, in the α-phase at 190 K in the current investigations. We find experimentally that profile evolution in the amorphous Pb wetting layer also exhibits nonclassical features, a coverage threshold and equilibration times that are very similar to the behavior in the Pb α-phase. The key common feature of these two structural phases appears to be their high densities, $\sim 4/3$ ML. The similar ring and coverage step profile propagation velocities for the two wetting layers are also orders of magnitude larger than would be expected based on observations of morphological changes and mass transport on Pb crystals [23,24]. These comparisons indicate that the origin of wetting layer mass transport must be similar in the profile evolution and island coarsening experiments, and distinct from Pb diffusion on bulk Pb substrates.

In summary, direct LEEM observations of nonclassical profile evolution in the Pb wetting layer on the Si(111) surface reveal unconventional convectionlike mass transport. Similar profile equilibration behavior is observed over a wide temperature range and at all coverages, despite an exceptional divergence of the equilibration time below $\theta_c \sim 4/3$ ML. As an alternative to standard diffusion models, which cannot account for this universal behavior, a model in which mass transport derives from the diffusion of thermally generated adatoms on top of the wetting layer has been shown to be applicable. The underlying mechanism that is responsible for these unusual results is likely also to be crucial to the remarkably efficient self-organization of uniform island height in this system. It is not clear if the monodisperse Pb quantum island height distribution on Si(111) is unique because of the unusual mass transport, or if similar mechanism or kinetic regime can be found in other systems. An answer to this question requires better understanding of mass transport as in the current work.

This work was supported by the Hong Kong Research Grants Council under grants HKUST600104 and HKUST600106. Work at the Ames Laboratory was supported by the Department of Energy-Basic Sciences under Contract DE-AC02-07CH11358.

[1] M. C. Tringides, M. Jałochowski, and E. Bauer, Phys. Today **60**, No. 4, 50 (2007).
[2] A. R. Smith *et al.*, Science **273**, 226 (1996).
[3] Z. Y. Zhang, Q. Niu, and C. K. Shih, Phys. Rev. Lett. **80**, 5381 (1998).
[4] L. Gavioli *et al.*, Phys. Rev. Lett. **82**, 129 (1999).
[5] K. Budde *et al.*, Phys. Rev. B **61**, R10 602 (2000).
[6] D.-A. Luh *et al.*, Science **292**, 1131 (2001).
[7] K. L. Man, Z. Q. Qiu, and M. S. Altman, Phys. Rev. Lett. **93**, 236104 (2004).
[8] V. Fournée *et al.*, Phys. Rev. Lett. **95**, 155504 (2005).
[9] M. Hupalo *et al.*, Surf. Sci. **493**, 526 (2001).
[10] W. B. Su *et al.*, Phys. Rev. Lett. **86**, 5116 (2001).
[11] H. Hong *et al.*, Phys. Rev. Lett. **90**, 076104 (2003).
[12] M. H. Upton *et al.*, Phys. Rev. Lett. **93**, 026802 (2004).
[13] A. Mans *et al.*, Phys. Rev. B **66**, 195410 (2002).
[14] T. L. Chan *et al.*, Phys. Rev. Lett. **96**, 226102 (2006).
[15] Li-Ying Ma *et al.*, Phys. Rev. Lett. **97**, 266102 (2006).
[16] M. Hupalo and M. C. Tringides, Phys. Rev. B **75**, 235443 (2007).
[17] C. A. Jeffrey *et al.*, Phys. Rev. Lett. **96**, 106105 (2006).
[18] J. Ma, X. Xiao, N. J. DiNardo, and M. M. T. Loy, Phys. Rev. B **58**, 4977 (1998), and references therein.
[19] C. M. Yim, K. L. Man, X. Xiao, and M. S. Altman, Phys. Rev. B **78**, 155439 (2008).
[20] A. T. Loburets, A. G. Naumovets, and Yu. S. Vedula, in *Surface Diffusion Atomistic and Collective Processes*, edited M. C. Tringides (Plenum, New York, 1997).
[21] L. Seehofer *et al.*, Phys. Rev. B **51**, 13 503 (1995).
[22] J. Slezak, P. Mutombo, and V. Chab, Phys. Rev. B **60**, 13 328 (1999).
[23] L. Kuipers and J. W. M. Frenken, Phys. Rev. Lett. **70**, 3907 (1993).
[24] K. Thürmer *et al.*, Phys. Rev. Lett. **87**, 186102 (2001).